Effects of Extrapolation Length δ on Switching Time and Coercive Field

Ahmad M. Musleh[a], Lye-Hock Ong[a]*, D.R. Tilley[a,b]

a Universiti Sains Malaysia, 11800 USM, Penang, Malaysia.

b Science Centre, University of Essex, Colchester CO4 4SQ, UK

The Landau free energy expression for a ferroelectric thin film studied by Tilley and Zeks (TZ-model) and the Landau-Khalatnikov dynamic equation are used to study the surface effects (represented by the extrapolation length $\pm\delta$) on properties of polarization reversal, namely switching time τ_S and coercive field e_C. Positive δ models a decrease of the local polarization at surfaces and negative δ an increase, with a smaller absolute value of δ giving a stronger surface effect. For positive δ, τ_S and e_C decrease with decreasing |δ| while for negative δ τ_S and e_C increase with decreasing |δ|. Strong surface effects, represented by smaller |δ|, are more profound in thin FE films.

* Corresponding author's email: onglh@usm.my

1 Introduction

Switching properties of ferroelectric (FE) thin films such as coercive field e_C, and switching time τ_s have attracted tremendous scientific and technological interests among the researchers over a long period of time. These properties are directly related to the application of FE films in nonvolatile FE random access memories (FeRAMs) where the speed of reversal of remanent polarization at low operating voltages is the main concern for the latest demand in producing devices which operate at reduced power consumption and at high switching speed [1, 2]. To support contributions from a large amount of experimental work, theorists have formulated a few models to elucidate these switching properties. The Kolmogorov-Avrami-Ishibashi (KAI) theory based on the Kolmogorov-Avrami theory [3-6] of crystal growth was first developed by Ishibashi *et al.*[7, 8] to explain the switching properties of FE film in terms of the statistics of domain coalescence. Du and Chen [9], then subsequently Tagantsev *et al.* [10], proposed a non-KAI model related to the work of Lohse *et al.* [11] concerning direct observations on switching in FE thin films [12, 13]. The model focuses on statistics of nucleation of domains and the results indicate that switching occurs region by region. Their results predict that in a particular region where switching has occurred, subsequent switching of the neighboring regions, as expected from KAI model, does not necessarily take place. The effects of surface on polarization reversal in a FE film are not discussed in these models.

In another approach, which is different from the classical nucleation reversal mechanism, Ishibashi [14] proposed a discrete model for the lattices of electric dipoles to describe behaviors of FE systems. His approach is based on the Landau-type-free energy for homogeneous [15] and inhomogeneous [14] systems. A periodic condition is implied in the finite inhomogeneous system but surface effects are ignored. In short, neither the models we have

mentioned in the preceding paragraph nor the discrete model of Ishibashi have taken the effects of surface on polarization reversal in FE film into consideration. Our primary aim in this paper is to present a model which is capable of simulating surface effects in switching. The model is illustrated with a selection of results from numerical explorations.

It is helpful to review a few experimental results. Arlt *et al.* [16] found that the Curie temperature of Barium Titanate increases above the bulk value with decreasing grain size. Similarly, for films of triglycine sulfate [17] and potassium nitrate [18], the Curie temperatures increase with decreasing film thickness. These results suggest enhancement of polarization at surfaces. Incidentally, density-function-theory calculations on ferroelectric films of lead titanate by Ghosez and Rabe [19] show a significant enhancement of polarization at the surfaces. On the other hand, Ishikawa *et al.* [20] have observed the phenomenon of lattice relaxation (suppression of polarization) at the surfaces of barium titanate and lead titanate films respectively. These and other experimental results indicate that a phenomenological theory should be capable of modeling both increases and decreases of polarization at film surfaces.

For static effects, particularly the calculation of critical temperatures and dielectric properties of films due to the enhancement or suppression of the polarization at the surfaces, the Tilley-Zeks (TZ) model [21], which is an extension of the Landau-Devonshire theory of bulk ferroelectrics, has been explored extensively [22, 23]. Here we extend the model to dynamic effects by adding a Landau-Khalatnikov equation of motion. The free energy of the TZ model is recalled and briefly discussed at the beginning of Section 2, then the extension to dynamical effects is introduced; in this paper we restrict attention to materials with a second-

order phase transition. Some representative numerical results are given in Section 3 and the general perspective we have gained from these and other results is outlined in Section 4.

2 Theory and Modeling

We consider a symmetric FE thin film of thickness L extending along the z axis, from $-L/2$ to $L/2$. As stated, the FE material is assumed to undergo a second-order phase transition. The model is one-dimensional with polarization and related physical quantities varying as a function of z, and the direction of polarization can be parallel to the film surfaces or perpendicular to the film surfaces for perovskite FE materials which have finite conductivity [24]; hence depolarization effects can be neglected. The surface density of the Landau-Devonshire free energy F for a film of thickness L is expressed as

$$\frac{F}{S} = \int_{-L/2}^{L/2} \left[\frac{A(T - T_C)}{2\varepsilon_o} P^2 + \frac{B}{4\varepsilon_o^2} P^4 + \frac{D}{2\varepsilon_o} \left(\frac{dP}{dz} \right)^2 - EP \right] dz + \frac{D}{2\varepsilon_o \delta} \left(P_-^2 + P_+^2 \right) \qquad (1)$$

Here P is the z-dependent polarization, T_C is the bulk transition temperature and A, B, and D are temperature-independent phenomenological coefficients, all taken to be positive. The factors of ε_0^{-1} and ε_0^{-2} are included so that A, B, and D have purely mechanical dimensions. The first two terms in the integrand will be recognized as the free energy for the corresponding bulk material; the implications of this free energy are discussed in standard texts [25]. The inhomogeneity of the film due to variation of P as function of distance z across the film thickness is represented by the term in $(dP/dz)^2$, so that D characterizes the 'stiffness' of the polarization. The final term in the integrand accounts for the interaction of the system with an external electric field E. It will be recalled that this term accounts completely for the electrostatic contribution to the free energy of the system. It is sometimes said that there should be additional terms describing coupling of the electric field to the

surface polarization values P_- and P_+. However, any such terms must arise from the EP integral, so they would require singular behavior in P at the surfaces. It may be that singularities could be found in a microscopic analysis, in which case they could be incorporated as an additional feature in eq. (1). However, it would not be correct to impose a singular structure on P in the present analysis since there is no clear reason to do so. The final term in eq.(1), in which P_- and P_+ are the values of P at the lower and upper surfaces, describes the increase or decrease of P at the surfaces by means of the extrapolation length δ. Since the equilibrium form of P is taken to correspond to a minimum of F/S, it can be seen straight away that a positive δ leads to values of P_- and P_+ smaller in magnitude than the value in the centre of the film, while negative δ leads to values larger in magnitude than the central value. Furthermore, since δ appears in the denominator, the surface effects become stronger as the absolute value of δ decreases. In the absence of a field E the free energy in eq. (1) is an even function of P, so that just as in the bulk material there are two equivalent minima of F, one with positive P and one with negative P. The gradient and surface terms in eq. (1) were introduced by Kretschmer and Binder [26] for a discussion of phase transitions in semi-infinite ferroelectrics; the extension of the analysis to films is due to Tilley and Zeks [21].

It will be helpful to discuss briefly the results obtained from eq.(1) without the electric-field term [21-23]. For positive values of δ, as stated, P is a maximum at the centre of the film; two examples are shown in Fig. 1 in which it is seen that the smaller values of δ do indeed give the larger surface effect. For negative δ, as seen in Fig. 2, P is largest at the surfaces and the surface enhancement is greater for smaller $|\delta|$. The corresponding results for the film critical temperature T_{CF} [21-23] are that for positive δ T_{CF} is below the bulk value T_C

and for negative δ it is above T_C, the difference between T_{CF} and T_C increasing with decreasing $|\delta|$.

With the electric field included, minimization of eq.(1) leads to the Euler-Lagrange equation

$$D\frac{d^2P}{dz^2} = A(T - T_C)P + \frac{B}{\varepsilon_0}P^3 - E \qquad (2)$$

with boundary conditions

$$\frac{dP}{dz} = \mp\frac{P}{\delta} \qquad \text{at} \quad z = \pm\frac{L}{2} \qquad (3)$$

For bulk ferroelectrics, P is independent of z so the derivative on the right-hand side of eq.(2) vanishes. The algebraic equation that results from equating the right-hand side to zero is used to calculate hysteresis loops and coercive fields of bulk materials [25]. Briefly, the equation is a cubic for P as a function of E and for T below T_c the graph of P is triple-valued for small E and single-valued for large E. The coercive field E_C is the dividing point between the two regions and the maximal hysteresis loop traces out the P graph between $+E_C$ and $-E_C$.

The extension of these bulk results to films using numerical integration of eq.(2) and eq.(3) was given by Tan et al.[27] We note from this the definition of E_C for a film. The average polarization is defined by $\overline{P} = L^{-1}\int P(z)dz$ and the graph of $\overline{P}$ versus E is drawn from the numerical results, the general form being similar to that for a bulk material. The points $\pm E_C$ are where this graph changes from single-valued to triple-valued; an example is given in Fig. 3 of Tan et al.[27]

For numerical calculations, it is convenient to scale all variables to dimensionless quantities. We let $\zeta = z/\xi_0$ and $l = L/\xi_0$ with $\xi_0^2 = D/AT_C$. It is seen from eq.(2) that at zero temperature ξ_0 is the characteristic length for the z dependence of P. Eq.(2) can also be used to model domain walls so that ξ_0 is a scale length for the domain-wall thickness. We let $t = T/T_C$, $p = P/P_0$ with $P_0^2 = \varepsilon_0 A T_C / B$ and $e = E/E_{C0}$ with $E_{C0}^2 = 4A^3T_C^3/27\varepsilon_0 B$. P_0 and E_{C0} are the equilibrium bulk polarization and the bulk coercive field at $T = 0\ K$ respectively.

As mentioned, we extend the TZ model to dynamics by adding the Landau-Khalatnikov (LK) equation of motion for P, namely $\gamma \partial P/\partial \tau = -\delta F/\delta P$, where τ is time and $\delta F/\delta P$ is the variational derivative. The characteristic time for variation of P is seen to be $\varepsilon_0 \gamma / AT_C \xi_0$ so we define a dimensionless time by $\tau_r = \tau(AT_C\xi_0/\varepsilon_0\gamma)$. The scaled LK equation is as follow

$$\frac{\partial p}{\partial \tau_r} = -\frac{\partial f}{\partial p} = (1-t)p - p^3 + \frac{d^2p}{d\zeta^2} + \frac{2}{3\sqrt{3}}e \tag{4}$$

where f is the reduced energy given by $f = BF/A^2T_C^{\,2}S\xi_0$. We use as a scalar order parameter the average polarization of the film defined as previously by $\bar{p} = \frac{1}{l}\int_{-l/2}^{l/2} p(\zeta)\, d\zeta$. The switching current is defined by $J = d\bar{P}/d\tau$ and the corresponding dimensionless quantity is

$$J_r = \frac{d\bar{p}}{d\tau_r} \tag{5}$$

It is useful to mention two ancillary quantities. The scaled bulk free energy is

$$f_B = \frac{t-1}{2}p^2 + \frac{1}{4}p^4 - \frac{2}{2\sqrt{3}}ep \tag{6}$$

and from this, the bulk coercive field can be derived:

$$e_C = (1-t)^{3/2} \tag{7}$$

We have now specified our model, and we proceed to discuss the numerical solutions of eqs.(2) to (4).

3 Numerical Method

We assume the polarization profile $p(\zeta)$ to be symmetric with respect to the film center $\zeta = 0$. Consequently, the surface polarizations p_+ and p_- are equal, such that $p(\zeta = 0) = p_C$ and $(dp/d\zeta) = 0$ at $\zeta = 0$. We find the polarization profile for $e = 0$ from the elliptic-function expressions derived in ref 22; examples of these profiles were shown in Fig. 1. The polarization profile of the system in a non-zero electric field is found by solving using the 4th order Runge-Kutta (RK) method to solve eq. 2 subject to the boundary conditions defined by eq. 3.[28] In zero electric field the polarization profiles obtained in this way agree with those calculated from the elliptic-function expressions[22]. To model switching, for example following a step-field change from $-E$ to $+E$, we integrate eq.(4) numerically by a finite difference technique. That is, the initial p profile ($\tau_r = 0$) is taken as that determined from the RK integration, then the field is switched to $+E$ and changes in $p(z)$ with τ_r are followed by finite differences.[28]

The most significant quantity in the polarization reversal is the switching time τ_S, which we define as the time taken when the switching current of eq. (5) falls to 10% of its maximum value [29, 30]. In all the simulations the initial form of p is taken as the negative zero-

field form, then at $\tau_r = 0$ a positive value of the electric field is applied and we study the evolution with time of the polarization profile $p(\zeta)$.

Results and discussion

The software we have described can be used for a wide variety of simulations. We now show some results for switching in a step field, with emphasis on the effect of the surface extrapolation length δ. As stated, the starting value of the profile $p(\zeta)$ is the negative form for zero field, then at time $\tau_r = 0$ the field is switched to a positive value e_F and we follow the time evolution of $p(\zeta)$, the average polarization $\overline{p}$ and quantities that can be derived from them. To set the scale for the dimensionless field, we note that eq. (7) shows that the bulk coercive field e_C decreases from 1 at $T = 0$ to 0 at the critical temperature $T = T_C$.

We start with positive values of the dimensionless extrapolation length δ_r. It will be recalled that positive δ_r corresponds to a decrease in magnitude of $p(\zeta)$ at the surfaces, and that the decrease is more marked for smaller values of δ_r. Fig.3 shows the evolution with time of $\overline{p}$ and the switching current $J_r = d\overline{p} / d\tau_r$ for various positive values of δ_r in a film of dimensionless thickness $l = 5.0$. At $\tau_r = 0$ the field is switched from zero to the high positive value $e = 10.0$. For $\delta_r = 100$ the surface effect is very weak, and as seen from Fig. 1 the profile $p(\zeta)$ is effectively flat across the film. Consequently the switching curves for this value of δ_r are indistinguishable from those for the bulk material. At the other extreme, $\delta_r = 0.1$ means a strong reduction of $p(\zeta)$ at the surfaces. Therefore, as seen, the starting

and finishing values of $\bar{p}$ are smaller in magnitude and the switching current is smaller. We have obtained similar curves to Fig. 3 for a range of values of the dimensionless thickness l. For a smaller value of l than that used for Fig. 3 there is, so to speak, less bulk material between the surfaces, so the reduction in $\bar{p}$ with decreasing δ_r seen in Fig. 3 sets in at higher values of δ_r.

As remarked, Fig. 3 shows the switching curves when the high value $e = 10.0$ is applied at $\tau_r = 0$. For comparison, Fig. 4 shows the curves when the switching is from $e = 0$ to $e = 1.1$. Here we might say that the switching force on $\bar{p}$ is much smaller and it is seen from Fig. 4 that the time scale for switching is much longer than in Fig. 3. Otherwise the qualitative comparisons between the three sets of curves in Fig. 4 are similar to those in Fig. 3.

Fig. 5 shows the evolution of average polarization $\bar{p}$ and switching current J_r of FE thin film with thickness $l = 0.72$ for negative δ_r of various magnitudes. In this case, as seen in Fig. 2, the value of $p(\zeta)$ is larger at the surfaces than in the center of the film, the enhancement being greater for δ_r of smaller magnitude. As in Figs 3 and 4, the starting profile $p(\zeta)$ is taken as the negative solution of eqs (2) and (3) with $E = 0$; thus the starting averages $\bar{p}$ in Fig. 5 are negative. The curves shown are for a step switch from $e = 0$ to $e = 10$ at $\tau_r = 0$. For the largest magnitude, $\delta_r = -100$, the profile $p(\zeta)$ is practically flat across the film. Consequently the switching curve starts at the zero-field bulk value $\bar{p} = -1$ and ends on the value $\bar{p} = 1.78$ found for the bulk in a field $e = 10$. For the smaller magnitude $\delta_r = -3.0$ both the starting and the finishing values of $\bar{p}$ are larger in magnitude than for $\delta_r = -100$; this is as expected because of the enhancement of $p(\zeta)$ at the surfaces. The same comments apply with more force for the smallest magnitude $\delta_r = -1.4$. It is seen

both from the main curves and from the inset to Fig. 5 that the peak switching current is larger and the switching takes longer for the smaller magnitudes of δ_r.

The switching time τ_S is a key quantity in this study and as remarked earlier we follow the usual definition that τ_S is the time at which the switching current J_r has fallen to 10% of its peak value. We have determined τ_S numerically for a range of values of thickness l and extrapolation length δ_r from numerous curves of the forms shown in Figs 3 to 5. Some example curves for the variation of τ_S with δ_r for two values of l are shown in Figs 6 and 7. Fig. 6 is concerned with positive δ_r, for which $p(\zeta)$ decreases at the surfaces and as seen from Figs 3 and 4 τ_S increases with increasing δ_r. It is seen that for given δ_r τ_S is smaller in the thinner film, for the obvious reason that there is less volume to switch. For negative δ_r, Fig. 7, $p(\zeta)$ increases at the surfaces and the mean polarization increases as δ_r increases toward zero. Consequently, as seen in Fig. 5 and shown in Fig. 7, τ_S increases as δ_r approaches zero. A feature that is surprising at first sight is that τ_S is larger in the thinner film, even though the ferroelectric volume is smaller. The reason is that the critical temperature of the thinner film is higher[21, 22] and because of this and the boundary conditions $p(\zeta)$ retains a high value across the film. Comparison of Figs 6 and 7 shows that the $\delta \to \infty$ limit of τ_S in the former is equal to the $\delta \to -\infty$ limit in the latter. This is easy to understand. As seen from eqs (1) and (3), although the usage of δ has become entrenched, the natural surface parameter in this model is in fact δ^{-1}. Continuity through $\pm\infty$ in δ is simply continuity through zero in δ^{-1}.

The second key quantity in switching is the coercive field e_{CF}. As mentioned earlier, this is found from the static equations (2) and (3) [27]; the extension to dynamics is not needed. However, it is so closely related to τ_S that we show in Figs 8 and 9 results that are complementary to those in Figs 6 and 7. For positive δ_r, Fig. 8, e_{CF} is larger in the thicker film and decreases as δ_r approaches zero. For negative δ_r, Fig. 9, e_{CF} is larger in the thinner film and increases as $|\delta_r|$ approaches zero. Finally, the $|\delta_r| \to \infty$ limits are the same in the two figures. These properties are similar to those discussed for τ_S and are explained in the same way.

Conclusions

We have extended the TZ model for ferroelectric thin films, which has been extensively studied for static effects, to include dynamic properties. We have applied our formalism to a study of switching in films. The model is phenomenological, and allows for either an increase or a decrease in the polarization profile $P(z)$ at the surfaces. This is important since both forms of behavior have been observed in experiments on different materials.

The results show that the effect of surfaces on switching time and coercive field is significant for small magnitudes of the extrapolation length δ, which means high surface effect; and it is especially so in thin films. It is of course beyond the scope of a phenomenological model to predict the value of δ from material properties; it is the surface parameter and could be determined, for example, by comparison of the film critical temperature with the bulk value [21, 22]. For an FE film with negative δ, although the critical

temperature increases with decreasing film thickness both the coercive field e_{CF} and switching time τ_S also increase. This may mean that the use of this type of material for small-sized memory devices is problematic. For films with positive δ, the critical temperature decreases with decreasing film thickness but the switching time τ_S and coercive field e_{CF} both also decrease, and these characteristics may be helpful for memory fabrication.

We should make a comment on the formalism. In order to illustrate the formalism clearly, we have restricted attention to materials in which the bulk phase transition is second-order. The earlier paper by Tan *et al.*[27] deals with the statics of both second-order and first-order materials. What we have added here is the treatment of the dynamics by means of the Landau-Khalatnikov equation and of course the numerical analysis of the resulting partial differential equation, eq (4). The extension of our analysis to first-order materials is straightforward.

The model presented here is concerned with single-domain switching, as might occur in a sample of small lateral dimension. Some recent experimental and theoretical studies have advanced understanding of the processes involved in polarization reversal by means of domain nucleation and lateral growth in thin films. Gruverman *et al.* [31] measured switching characteristics in 180 nm thick films of PZT. They compared measurements of switching current versus time with piezoresponse force microscopy (PFM) images of the evolution of the domain structure in time, finding significant differences between samples of different lateral dimension (areas on the scale of 1.5 to 25 μm^2). This work has been extended to a study of the nucleation and evolution of vortex domains [32, 33]. Variation with lateral dimension was also the emphasis in the study by Jung *et al.* [34] of switching kinetics and hysteresis loops in PZT films. Scanning transmission electron microscopy (STEM) studies of

the domain patterns in free-standing $BaTiO_3$ films with thicknesses varying between 70 and 530 nm have been reported by Schilling *et al.*[35], and these bring out the significance of strain effects.

Acknowledgments

The work is funded by the SAGA grant, Academy of Sciences Malaysia (Grant No: 304/PFIZIK/653018/A118). We sincerely thank Prof. Junaidah Osman for some useful comments.

References

[1] J. F. Scott, *Ferroelectric memories* (Springer, Berlin; New York, 2000).

[2] M. Dawber, K. M. Rabe, and J. F. Scott, Rev. Mod. Phys. **77,** 1083 (2005).

[3] A. N. Kolmogorov, Izv. Akad. Nauk USSR., Ser Math. **3,** 355 (1937).

[4] M. Avrami, J. Chem. Phys. **7,** 1103 (1939).

[5] M. Avrami, J. Chem. Phys. **8,** 212 (1940).

[6] M. Avrami, J. Chem. Phys. **9,** 177 (1941).

[7] H. Orihara, S. Hashimoto, and Y. Ishibashi, J. Phys. Soc. Jpn. **63,** 1031 (1994).

[8] S. Hashimoto, H. Orihara, and Y. Ishibashi, J. Phys. Soc. Jpn. **63,** 1601 (1994).

[9] X. Du and I-W. Chen, Appl. Phys. Lett. 72, 1923 (1998).

[10] A. K. Tagantsev, I. Stolichnov, N. Setter, J. S. Cross, and M. Tsukada, Phys. Rev. B **66,** 214109 (2002).

[11] O. Lohse, M. Grossmann, U. Boettger, D. Bolten, and R. Waser, J. Appl. Phys. **89,** 2332 (2001).

[12] E. L. Colla, S. Hong, D. V. Taylor, A. K. Tagantsev, N. Setter, and K. No, Appl. Phys. Lett. **72,** 2763 (1998).

[13] C. S. Ganpule, V. Nagarajan, H. Li, A. S. Ogale, D. E. Steinhauer, S. Aggarwal, E. Williams, R. Ramesh, and P. De Wolf, Appl. Phys. Lett. **77,** 292 (2000).

[14] Y. Ishibashi, J. Phys. Soc. Jpn. **59,** 4148 (1990).

[15] Y. Ishibashi, Jpn. J. Appl. Phys. **31,** 2822 (1992).

[16] G. Arlt, D. Hennings, and G. de With, J. Appl. Phys. **58,** 1619 (1985).

[17] A. Hadni, R. Thomas, S. Ungar, and X. Gerbaux, Ferroelectrics **47,** 201 (1983).

[18] J. F. Scott, H. D. Duiker, P. D. Beale, B. Pouligny, K. Dimmler, M. Parris, D. Butler, and A. S. Athems, Physica B+C **150,** 160 (1988).

[19] P. Ghosez and K. M. Rabe, Appl. Phys. Lett. **76,** 2767 (2000).

[20] K. Ishikawa and T. Uemori, Phys. Rev. B **60,** 11841 (1999).

[21] D. R. Tilley and B. Zeks, Solid State Commun. **49,** 823-827 (1984).

[22] L. H. Ong, J. Osman, and D. R. Tilley, Phys. Rev. B **63,** 144109 (2001).

[23] W. L. Zhong, B. D. Qu, P. L. Zhang, and Y. G. Wang, Phys. Rev. B **50,** 12375 (1994).

[24] Y. Watanabe, Phys. Rev. B **57,** 789 (1998).

[25] M. E. Lines and A. M. Glass, *Principles and Applications of Ferroelectrics and Related Materials.* Oxford: Clarendon Press (1977).

[26] R. Kretschmer and K. Binder, Phys. Rev. B **20,** 1065 (1979).

[27] E-K Tan, J. Osman and D.R. Tilley, Solid State Comms **117**, 59 (2001).

[28] W. H. Press, B. P. Flannery, S. A. Teukolsky and W. T. Vetterling, *Numerical Recipes, The Art of Scientific Computing.* Cambridge: Cambridge University Press (1986).

[29] S. E. Cummins, J. Appl. Phys. **36,** 1958 (1965).

[30] M. Omura and Y. Ishibashi, Jpn. J. Appl. Phys. **31,** 3238 (1992).

[31] A. Gruverman, D. Wu ans J.F. Scott, Phys. rev. Lett. 100, 097601 (2008)

[32] A. Gruverman, D. Wu, H-J Fan, I. Vrejoiu, M. Alexe, R.J. Harrison and J.F. Scott, J. Phys.: Condens. Matter 20, 342201 (2008)

[33] J.F. Scott, A. Gruverman, D. Wu, I. Vrejoiu and M. Alexe, J. Phys.: Condens. Matter 20, 425222 (2008)

[34] D.J. Jung, K. Kim and J.F. Scott, J. Phys.: Condens. Matter 17, 4843 (2005)

[35] A. Schilling, T.B. Adams, R.M. Bowman, J.M. Gregg, G. Catalan and J.F. Scott, Phys. rev. B 74, 024115 (2006)

Figure Captions

Fig.1 Polarization profile for positive extrapolation length $\delta_r = 0.1$ (solid curve); $\delta_r = 3.0$ (dashed curve); $\delta_r = 100$ (dotted curve) $e = 0.0$, $l = 5.0$ and t =0.0.

Fig.2 Polarization profile for negative extrapolation length $\delta_r = -1.4$ (solid curve); $\delta_r = -3.0$ (dashed curve); $\delta_r = -100$ (dotted curve) $e = 0.0$, $l = 5.0$, t =0.0.

Fig.3 Time dependence of average polarization $\overline{p}$ for positive extrapolation lengths $\delta_r = 0.1$ (solid curve); $\delta_r = 3.0$ (dashed curve); $\delta_r = 100$ (dotted curve), $l = 5.0$, $t = 0.0$, $e = 10.0$. The inset shows the corresponding switching current.

Fig.4 Time dependence of average polarization $\overline{p}$ for positive extrapolation lengths $\delta_r = 0.1$ (solid curve); $\delta_r = 3.0$ (dashed curve); $\delta_r = 100$ (dotted curve), $l = 5.0$, $t = 0.0$, $e = 1.1$. The inset shows the corresponding switching current.

Fig.5 Time dependence of average polarization $\overline{p}$ for negative extrapolation lengths $\delta_r = -1.4$ (solid curve); $\delta_r = -3.0$ (dashed curve); $\delta_r = -100$ (dotted curve), $l = 0.72$, t = 0.0, e = 10.0. The inset shows the corresponding switching current.

Fig.6 Switching time versus positive extrapolation length, for film thicknesses l = 0.72 (O), and 5.0 (Δ) at t = 0.0, e = 10.0.

Fig.7 Switching time versus negative extrapolation length, for film thicknesses l = 0.72 (O), and 5.0 (Δ) at t =0.0, e=10.0. The inset shows the zoom-in view for l = 5.0 (Δ).

Fig.8 Coercive field versus positive extrapolation length for film thicknesses l = 0.72 (O), and 5.0 (Δ) at t = 0.0.

Fig.9 Coercive field versus negative extrapolation length for film thicknesses l = 0.72 (O), and 5.0 (Δ) at t = 0.0. The inset shows the zoom-in view for l = 5.0 (Δ).

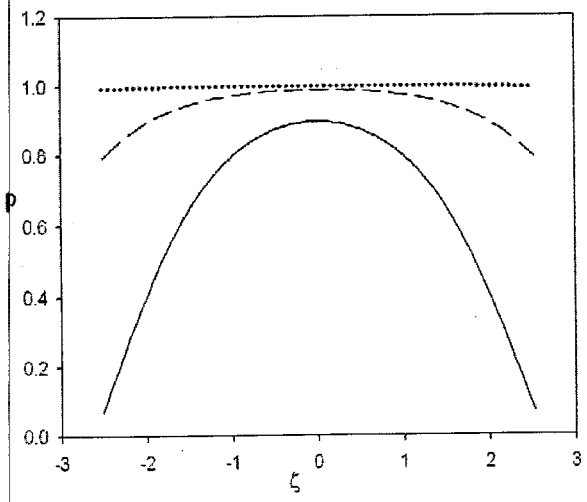

Fig. 1

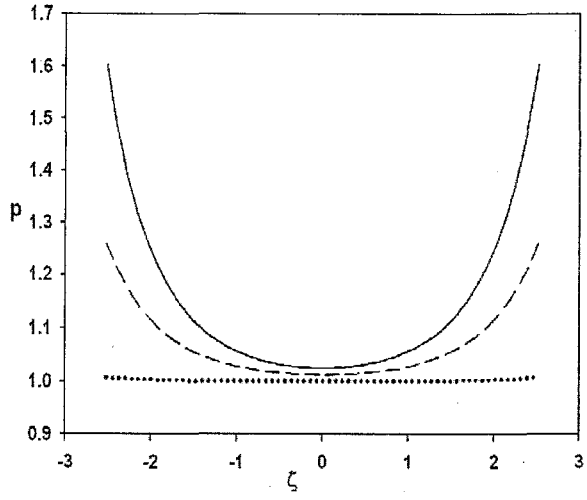

Fig. 2

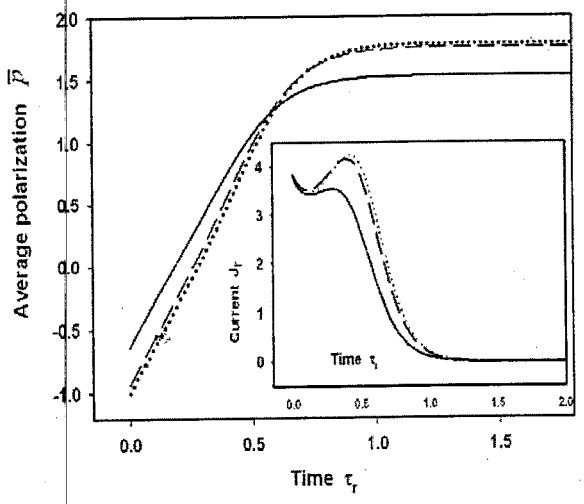
Average polarization $\overline{p}$
2.0
1.5
1.0
0.5
0.0
-0.5
-1.0
0.0
0.5
1.0
1.5
Time τ_r
Current J_r
4
3
2
1
0
Time τ_r
0.0
0.5
1.0
1.5
2.0

Fig. 3

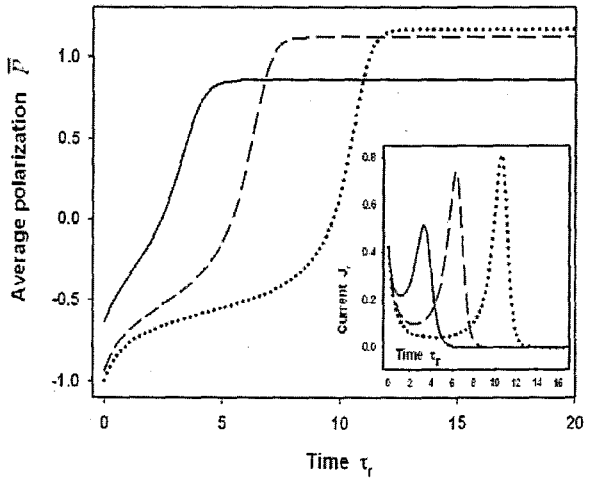
Average polarization $\overline{P}$
1.0
0.5
0.0
-0.5
-1.0
0
5
10
15
20
Time τ_r
Current J_r
0.8
0.6
0.4
0.2
0.0
Time τ_r
0
2
4
6
8
10
12
14
16

Fig. 4

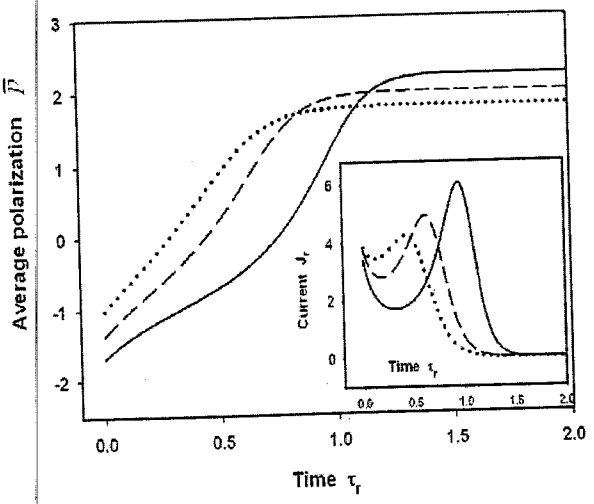
Average polarization $\overline{P}$
3
2
1
0
-1
-2
0.0
0.5
1.0
1.5
2.0
Time τ_T
Current J_T
6
4
2
0
Time τ_T
0.0
0.5
1.0
1.5
2.0

Fig. 5

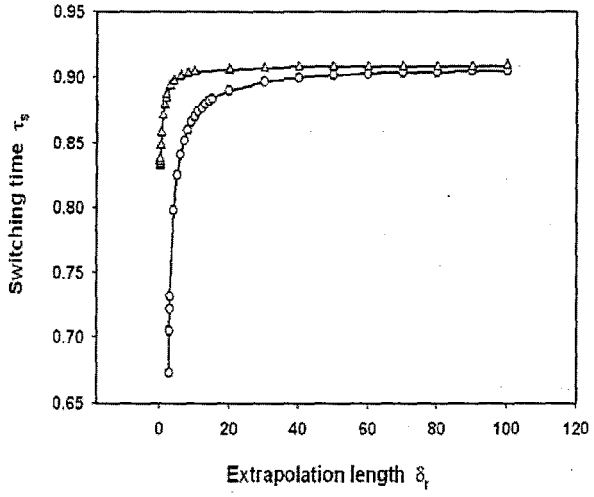
0.95
0.90
0.85
0.80
0.75
0.70
0.65
Switching time τ_s
0
20
40
60
80
100
120
Extrapolation length δ_t

Fig. 6

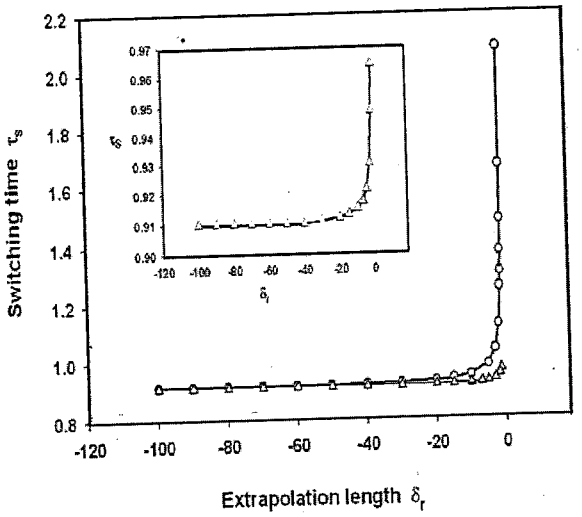
Switching time τ_s
Extrapolation length δ_f
2.2
2.0
1.8
1.6
1.4
1.2
1.0
0.8
-120
-100
-80
-60
-40
-20
0
0.97
0.96
0.95
0.94
0.93
0.92
0.91
0.90

Fig. 7

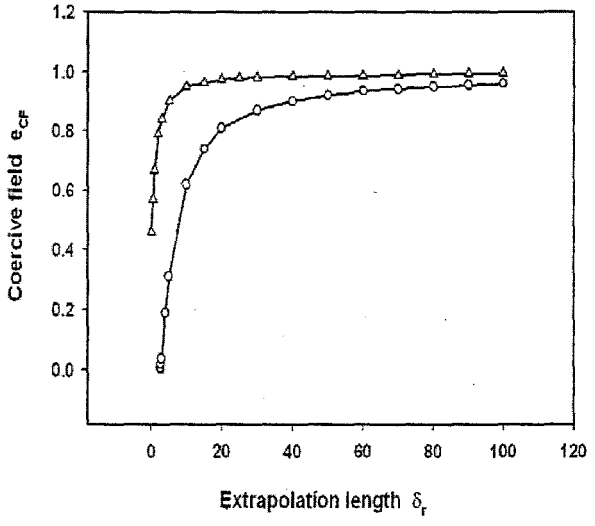
1.2
1.0
0.8
0.6
0.4
0.2
0.0
Coercive field e_{cF}
0
20
40
60
80
100
120
Extrapolation length δ_r

Fig. 8

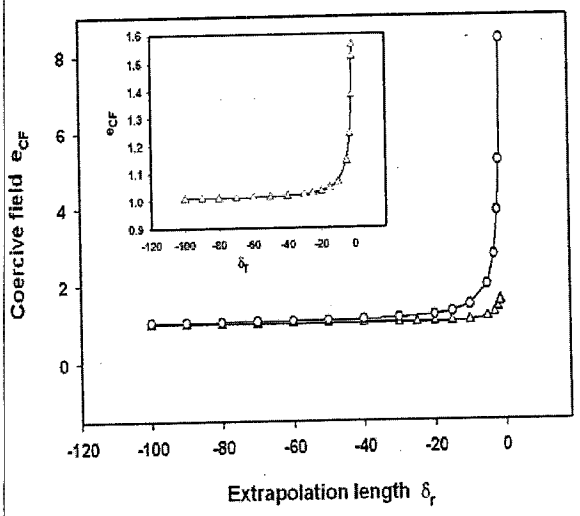
Coercive field e_{CF}
Extrapolation length δ_r
0
2
4
6
8
-120
-100
-80
-60
-40
-20
0
e_{CF}
δ_r
0.9
1.0
1.1
1.2
1.3
1.4
1.5
1.6

Fig. 9